



Complementary screening for quantum spin Hall insulators in two-dimensional exfoliable materials

Davide Grassano ^{1,*}, Davide Campi^{1,2,3}, Antimo Marrazzo ^{1,4} and Nicola Marzari¹¹*Theory and Simulations of Materials (THEOS) and National Center for Computational Design and Discovery of Novel Materials (MARVEL), École Polytechnique Fédérale de Lausanne, CH-1015 Lausanne, Switzerland*²*Dipartimento di Scienza dei Materiali, Università di Milano-Bicocca, Via Cozzi 53, 20125 Milano, Italy*³*Bicocca Quantum Technologies (BiQuTe) Centre, I-20126 Milano, Italy*⁴*Dipartimento di Fisica, Università di Trieste, I-34151 Trieste, Italy*

(Received 6 May 2022; revised 21 June 2023; accepted 10 August 2023; published 13 September 2023)

Quantum spin Hall insulators are a class of topological materials that has been extensively studied during the past decade. One of their distinctive features is the presence of a finite band gap in the bulk and gapless, topologically protected edge states that are spin-momentum locked. These materials are characterized by a \mathbb{Z}_2 topological order where, in the two-dimensional case, a single topological invariant can be even or odd for a trivial or a topological material, respectively. Thanks to their interesting properties, such as the realization of dissipationless spin currents, spin pumping, and spin filtering, they are of great interest in the field of electronics, spintronics, and quantum computing. In this work we perform a high-throughput screening of quantum spin Hall insulators starting from a set of 783 two-dimensional exfoliable materials, recently identified from a systematic screening of the Inorganic Crystal Structure Database, Crystallography Open Database, and Materials Platform for Data Science databases. We find four \mathbb{Z}_2 topological insulators and seven direct gap metals that have the potential of becoming quantum spin Hall insulators under a reasonably weak external perturbation.

DOI: [10.1103/PhysRevMaterials.7.094202](https://doi.org/10.1103/PhysRevMaterials.7.094202)

I. INTRODUCTION

Topological states of matter [1] have been one of the main subjects of study for condensed matter physicists in the past decade. One of the driving aspects lies in the robustness of many properties of topological materials, whose existence can be directly related to a specific set of topological invariants [2–4]. In the case of insulators, the ground state of a topologically trivial material can be connected to the one of an atomic insulator or vacuum by a smooth adiabatic deformation of its Hamiltonian, while for a topologically nontrivial material, this cannot happen without closing a gap in its band structure. Among the possible classifications of topological insulators, quantum spin Hall insulators (QSHIs) represent a class of materials protected by time-reversal (TR) symmetry where the quantum spin Hall effect (QSHE) [5] can be realized. This is made possible by the presence of a finite bulk gap and spin-polarized gapless helical hedge states [6] that can sustain dissipationless spin currents [1] thanks to the absence of backscattering forbidden by TR. Other interesting properties arise from spin-momentum locking [7], which allows for the possibility to realize spin filtering [8], injection, detection [9], and pumping [3], all of which make QSHIs of great interest for the realization of spintronic devices. It has also been shown that magnetic confinement can be used in order to realize qubits on the surface of a QSHI [10], making these materials promising for applications in quantum computing. The need for finding new topological materials, and in particular QSHIs, is further accentuated by the recent surge in

high-throughput studies [11–17], especially when related to easily exfoliable materials [18–21].

QSHIs can be identified through a \mathbb{Z}_2 invariant which can be either even (0) or odd (1), as first proposed by Kane and Mele, that showed that a Dirac cone with a gap opened by spin-orbit coupling (SOC) can lead to a topologically nontrivial order [5,22]. This concept has later been extended as, in general, a QSHI can be obtained whenever a band inversion takes place, as in the paradigmatic cases of, e.g., HgTe quantum dots [23,24] and $\text{Bi}_{1-x}\text{Sb}_x$ [25]. A nontrivial \mathbb{Z}_2 invariant can emerge naturally due to the material intrinsic band structure, or can be induced by a perturbation, such as the application of strain or electric fields or the interaction with a substrate [26–30]. Hence, a trivial insulator can be driven into a topological insulator and vice versa, leaving open the possibility to realize a topological transistor [31,32]. While for two-dimensional (2D) materials a single invariant is sufficient in order to describe their topology with respect to the QSHE, it has been shown that for three-dimensional (3D) materials a set of four invariants is required, leading to the possibility of weak or strong \mathbb{Z}_2 topological insulators [33]. It has also been shown that the topology of a system can often be related to its symmetries [34–38]. For example, in the case of QSHIs with inversion symmetry, the \mathbb{Z}_2 topological invariant can be computed easily by calculating the eigenvalues of the parity operator at the time-reversal invariant momenta (TRIM) points of the Brillouin zone (BZ) [25].

In this work we perform a complementary screening to that of Marrazzo *et al.* [12], by using a set of 2D materials from Ref. [39], in which 1252 monolayers, exfoliable from their layered (typically van der Waals bonded) parents, have been added to the initial 2D portfolio [18] used in Ref. [12].

*davide.grassano@epfl.ch

We set out with this, the aim of identifying all the 2D \mathbb{Z}_2 topological insulators present in this set, analyzing all the materials with less than 40 atoms per unit cell, with the exception of lanthanides due to their typically complex, correlated electronic structure [40]. We also identify direct gap metals (DGMs) which can serve as \mathbb{Z}_2 candidates, by calculating the invariant for materials where the valence and conduction band manifolds are separated by a direct gap (DG), but where the indirect gap (IG) is negative.

II. METHODS

All the density-functional theory (DFT) calculations performed in this work use the QUANTUM ESPRESSO (QE) [41,42] distribution. We perform fully relativistic calculations with SOC, using the Perdew, Burke, and Ernzerhof (PBE) pseudopotentials [43] from the ONCVSP (v0.4) set [44] contained in the PSEUDODOJO library [45]. For every calculation we use a kinetic cutoff, high enough to ensure that the uncertainty on the energy eigenvalues is lower than 5 meV. In order to properly account for low-gap and metallic systems, a Fermi-Dirac smearing of 5 meV is used. For the initial self-consistent calculations we use a \mathbf{k} -point mesh of density 0.2 \AA^{-3} , which is refined to 0.1 \AA^{-3} for QSHI candidates. All the calculations have been performed assuming a nonmagnetic ground state, and magnetism has been later checked for the selected candidates following the same approach used in Ref. [18].

The topological invariants are computed either from an analysis of the band structures at the TRIM points or using the Z2PACK package [46], for which we set the maximum number of \mathbf{k} -points per line to 200, and the lowest acceptable distance between lines to 10^{-7} . The threshold on the hybrid Wannier charge centers (HWCC) [47] position variation per step on a line (`pos_tol`) is set to 0.01, the threshold on the relative movement of the HWCCs position between neighboring (`move_tol`) to 0.3, and the threshold for the distance between the middle of the largest gap in a line and the position of the neighboring HWCC (`gap_tol`) to 0.3.

For the QSHI found, we also perform a hybrid functional calculation, using HSE06 [48]. We find that in order to obtain a properly converged Wannierization of the system, a very dense $32 \times 16 \times 1$ \mathbf{k} -point mesh with a $4 \times 2 \times 1$ \mathbf{q} -point mesh has to be used. The Wannierized wave functions are then used to compute the topological invariant and edge states, in order to confirm whether the system remains a topological insulator.

Screening procedure

The original set of material of which we explore the properties is derived from the Inorganic Crystal Structure Database [49,50], Crystallography Open Database [51], and MPDS [52] databases, by identifying 2D exfoliable materials, starting from experimentally known bulk structures using van der Waals (vdW) DF2-C09 DFT calculations [18]. First we exclude all materials containing lanthanides, due to the inaccuracy of plain DFT pertaining calculations with these atoms caused by the presence of strongly correlated electrons [40]. For the remaining 603 materials, compared to the 1306 structures studied in Ref. [12] by Marrazzo *et al.*, we follow

two strategies for the identification of QSHIs in order to minimize the usage of computational resources. For the ones with inversion symmetry we use the formula given by Fu and Kane [25],

$$(-1)^\nu = \prod_i \delta_i, \quad \delta_i = \prod_{m=1}^N \xi_{2m}(\Gamma_i), \quad (1)$$

where ν is the \mathbb{Z}_2 topological invariant, ξ_{2m} is the eigenvalue of the parity operator calculated for a couple of TR-paired bands, and Γ_i are the TRIM points, of which there are four for a 2D material, defined as

$$\Gamma_i = -\Gamma_i + \mathbf{G}, \quad (2)$$

with \mathbf{G} being any reciprocal lattice vector. For a 2D material, four TRIM points can be found at the coordinates (0, 0), (0, 0.5), (0.5, 0), and (0.5, 0.5) expressed in units of the reciprocal lattice vector. Given the formula in Eq. (1), the most computationally efficient route for materials that have inversion symmetry is to first calculate the band structure at the TRIM points to determine the topological invariants. Materials with $\nu = 0$ are discarded, while for those with $\nu = 1$ we proceed with a band structure calculation along the high-symmetry lines. The result can either be a material with finite DG on the entire \mathbf{k} -point path, or one with a zero DG. The latter is discarded as a metal or semimetal without an isolated valence band manifold, while the former can either be a QSHI if the IG—defined as the difference between the minimum of the conduction band and the maximum of the valence band—is positive, or a DGM if the IG is negative. The values of the DGs and IGs are further corroborated by analyzing the band structure computed on a dense uniform \mathbf{k} -point grid with a spacing of 0.015 \AA^{-1} . We discard materials that are DGM with an IG lower than -0.15 eV , as attempting to drive such a material to a topological phase would be hardly feasible. The same band structure on the dense uniform grid is also used to derive the density of states (DOS) for the materials studied.

If inversion symmetry is not present, we follow a different route, by determining the DG and IG first through a band structure calculation and discarding the metals and semimetals without a finite DG. We then use the Z2PACK package, which tracks the positions of one-dimensional HWCCs across half of the BZ, in order to compute the topological invariant [53]. The package acts as an automation tool, which interfaces a DFT code (QE in our case) with WANNIER90 [54] in order to calculate the HWCC positions on a progressively denser grid of \mathbf{k} -points. If one of the convergence criteria of Z2PACK, with the parameters mentioned before, is not satisfied, then the material is discarded. If the result of the calculation is a nontrivial topological invariant, the material is then classified as a QSHI or DGM following the same criteria mentioned for the inversion-symmetric cases, where the direct and indirect gaps are then checked again from the band structures on a dense \mathbf{k} -point grid also used for the DOS.

Finally, for the selected candidates we assess the dynamical stability by computing the full phonon dispersion by means of density-functional perturbation theory [55], and we check the nonmagnetic ground state assumption comparing the energy of the nonmagnetic ground state with different possible ferromagnetic, antiferromagnetic, and ferrimagnetic

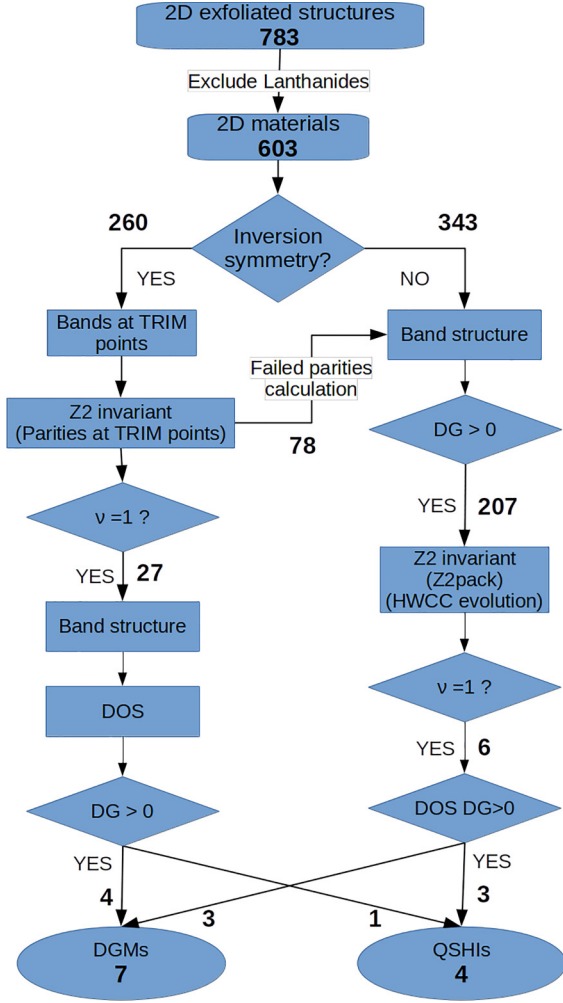


FIG. 1. Workflow adopted for the high-throughput screening of the QSHIs. Starting from 783 structures presented in Ref. [39], we proceed to a study of the \mathbb{Z}_2 topological invariant following two branches, depending on the presence of inversion symmetry in the material. The steps in both branches are organized as to limit the usage of resources, by performing the lowest cost screenings first in each branch.

configurations following the same procedure adopted in Ref. [18]. A flowchart describing the entire high-throughput calculation is shown in Fig. 1. The entire process has been automated using AiiDA [56,57], a workflow-managing infrastructure which enables us to keep track of the provenance at every computational step. The data produced in this work, including both the results and the entire provenance tree, has been made available on the Materials Cloud as Ref. [58].

III. RESULTS AND DISCUSSION

We start our screening from a set of 783 2D exfoliable structures taken from Ref. [39], which are reduced to 603 after removing materials containing lanthanides. The set is further divided into two groups of 260 and 342 structures with and without inversion symmetry. For the inversion symmetric materials, we compute the eigenvalues of the parity operator ξ_{2m} , the calculation of which can sometimes fail due to limitations

TABLE I. Table containing a collection of direct (DG) and indirect (IG) band gaps (derived from the final calculations on a dense \mathbf{k} -point grid), binding energies (E_B), and previous literature references for the QSHIs and DGMs identified. In bold are the materials from the current work, while in normal text those in the previous work by Marrazzo *et al.* [12] (in absence of strain). For HgNS, both the PBE and HSE gap (in parentheses) are reported.

	Formula	DG (meV)	IG (meV)	E_B (meV)	Ref.
QSHI	HfBr	233	48	15.8	[65,66]
	HfTe₅	299	171	16.5	[69]
	HgNS	7 (38)	7 (38)	19.4	
	ZrTe₅	281	220	19.4	[69]
	Pt ₂ HgSe ₃	178	142	60.2	[72]
	RhTaTe ₄	67	67	26.4	[73]
	AsCuLi ₂	65	58	62.7	
	TiCu ₂ Te ₃	6	5	44.0	
	IrNbTe ₄	40	37	27.1	[73]
	Bi	656	578	17.9	[18]
	TiNi	20	20	14.6	[18,74]
	In ₂ ZnS ₄	7	5	36.1	
TaIrTe ₄	15	15	25.8	[73]	
DGM	BaCr₂N₂O₈	19	-124	11.0	
	VBr₃	33	-99	15.1	
	FePO₄(CH₃)	11	-58	18.8	
	HfCl	264	-166	14.8	[65]
	Fe₂O₃	17	-21	6.4	
	MoI₂S₂	47	-117	14.4	
	Mo₂Ta₂O₁₇	17	-36	10.0	
	WTe ₂	738	738	24.7	[18,32]
	MoTe ₂	107	-259	24.5	[18,32]
	ZrBr	45	-19	15.6	[11,65]
ZrCl	64	-196	14.7	[65]	

in the code to handle nonsymmorphic space groups, or due to the accuracy threshold imposed for the calculation of the trace of the representation for each group of bands. A total of 78 out of these 260 TRIM point calculations failed and were hence recalculated using Z2PACK. Of the 182 successful calculations, 27 resulted in a nontrivial topological invariant $\nu = 1$. We then performed band structure calculations along the high-symmetry path [59], from which we excluded 22 metallic materials and identified 1 QSHI (HfBr) and four direct gap metals (DGMs).

On the 343 + 78 remaining structures (the noninversion symmetric ones and those with failed parity calculations), the band structure calculations show that 207 materials have a DG greater than 0; for them we proceed with Z2PACK calculations that identify three QSHIs (ZrTe₅, HgNS, HfTe₅) and three DGMs. The summary of the data for every material is reported in Table I, while a more detailed report is given in the Supplemental Materials [60], together with the crystal structure and band structure of the material identified and a plot of the HWCC for every Z2PACK calculation.

A summary for all the materials analyzed in the present work, together with those of the previous screening by Marrazzo *et al.* [12] (in absence of strain), is shown in Fig. 2, where the QSHIs are highlighted. In the figure, all materials with a negative IG have been put on the $y = 0$ axis in order

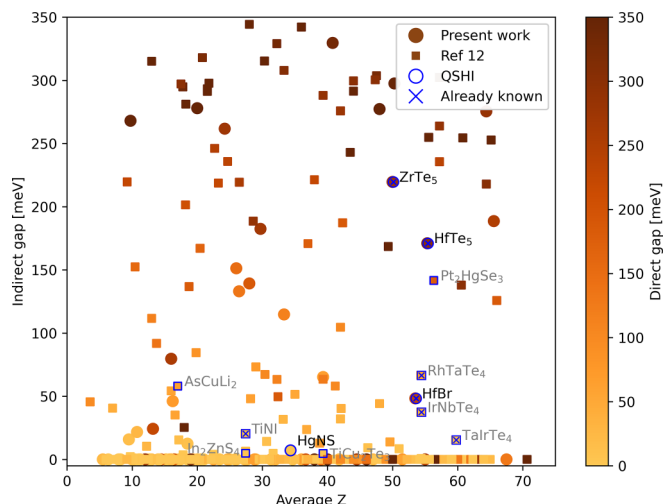


FIG. 2. Plot of the direct (color scale) and indirect (y-axis) band gaps in the presence of SOC for all the material screened in the current work (circles) and in the previous work of Marrazzo *et al.* [12] (squares). Materials with negative IGs have been given a zero value. The DG for each material is given using the color scale on the right. QSHIs identified by the present screening effort and that of Ref. [12] are highlighted using a blue contour to the circle or squares. Materials already known in the literature are also highlighted with a cross mark.

to emphasize QSHIs and DGMs, especially with regard to the magnitude of the DG and IG, as these two parameters can be used to determine the range of temperatures at which a device could operate [61].

The interest in DGMs with a nontrivial ν is twofold. First, it is possible that, given the limitations of DFT-PBE calculations, the band gap of the material is being underestimated and, using more appropriate methods (such as many-body perturbation theory in the GW approximation [62]), a material that was computed to be a DGM with DFT-PBE could actually result to be a QSHI. It is worth highlighting that the opposite could also be possible, where a material that is estimated to be a QSHI within DFT-PBE could end up being a trivial insulator in a GW calculation (as discussed for the case of TiNi in Ref. [12]). Second, a DGM could be driven into a \mathbb{Z}_2 topological state through an external perturbation that could open a gap in the material without driving a band inversion [29,30]. To this end, it is important to look at both the IG and DG of the material. The former is related to how strong a perturbation needs to be in order to drive the material in a semiconducting state, while the latter gives us an idea of how likely it is that a gap could be opened without causing band inversion or driving the material into a metallic state. Indeed, the higher the DG of a material, the more difficult it will be to close it. For this reason, DGMs with small negative IG and large DG are prime candidates for further studies; a visual summary of the direct and indirect gap of the DGMs is shown in Fig. 3. Among the various possible perturbations that could open the gap, the most interesting ones, from the standpoint of applications in a device, would be gating or electric fields [27], the interaction with a substrate [63], and/or the application of strain [64].

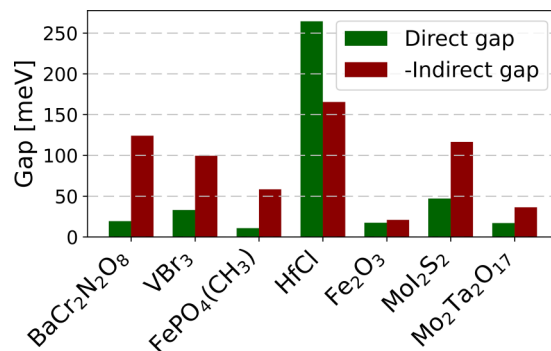


FIG. 3. Plot of the direct and indirect band gaps of the DGMs identified. The criteria used are that the material has to exhibit DG > 0 (which allows for the calculation of \mathbb{Z}_2 on an isolated manifold) and a negative IG < 300 meV. These materials would become QSHIs in the presence of perturbations such as strain, substrate interactions or an electric field capable of opening the IG without causing a band inversion.

For all the materials found, we searched the current literature to determine which QSHIs were already known, and which one are novel to this study. We find that among the four QSHIs identified, three were already known, namely, the two tellurides of hafnium and zirconium, and hafnium bromide. HfBr [65,66] was already known both for being an easily exfoliable material and for its topological properties in its 2D and 3D forms. This material has a DG of 233 meV and an IG of 48 meV, making it a good candidate for experiments and possible device realization. It should also be noted that this material belongs to a broader class of transition-metal halides MX ($M = \text{Zr, Hf}$, $X = \text{Cl, Br}$) which has already been predicted to host topological properties. Furthermore, several class of similar honeycomb materials have also been predicted to host topological states such as transition metal carbides MC ($M = \text{Ti, Zr, Hf}$) [67] and transition metal compounds MM' ($M = \text{Ti, Zr, Hf}$) ($M' = \text{Bi, Sb}$) [68].

HfTe₅ (ZrTe₅) [69] are two pentatellurides, both of which have large DGs of 300(281) meV and IGs of 171(220) meV, making them both very good candidates for QSHIs applications at room temperature. Interestingly, as shown by Weng *et al.* [69], the presence of a band inversion in these materials comes mainly from the nonsymmorphic features of their space group which, together with the presence of two nonequivalent Te atom chains, drives the ordering of the bands at Γ . At the same time, the symmetries of the space group give rise to fourfold degenerate bands at the TRIM points, two with even and two with odd parity, such that the presence of SOC will only open a gap in a band structure that would otherwise be metallic, but will preserve the product of parity eigenvalues at the TRIM points. These pentatellurides have also been proposed for the realization of the quantum anomalous Hall effect, when the transition metal Hf/Zr is substituted for a rare-earth metal which could induce a magnetic ordering in the material, breaking time-reversal symmetry [69,70].

HgNS is a compound which has not been discussed in the literature for its topological properties. Its direct and indirect gaps are both of 7 meV. Such a low gap, in between that of silicene (1.4 meV) and germanene (23.8 meV), precludes

room temperature applications. Nevertheless, at the gap, situated along the Γ - Y direction, the material shows a linear band dispersion akin to that of germanene at K when SOC is taken into account. The similarity between the two systems opens the possibility for a multitude of studies, such as the effect of an electric field on the gap and band inversion [27,28] or the possibility for optoelectronic applications in THz devices [71]. Given that HgNS would constitute a new QSHI, we also study it using the hybrid HSE06 functional as described in the methods. We find, as expected, that the effect of the hybrid is that of increasing the gap in the material. We can also observe from the band structure shown in the Supplemental Material [60] that the gap opening goes against the band inversion, moving the quasi-linear crossing toward the edge of the zone, but is not strong enough to drive the material to a trivial state. Hence, we find that HgNS is still a QSHI, as corroborated by the HWCCs evolution and edge state calculations shown in the Supplemental Material [60], even when a hybrid functional is used, and the gap increases from 7 meV to 38 meV.

Among the DGMs, the most promising ones are Fe_2O_3 and $\text{Mo}_2\text{Ta}_2\text{O}_{17}$, with small IGs of -21 and -36 meV, respectively. The small negative IGs indicate that it could be feasible to force those from being DGM to a QSHI by acting via strain, electric field, or other perturbations. There is also HfCl, which, like HfBr, is a transition metal halide and has been studied in Ref. [65], in which the material is identified as a semimetal for both PBE and PBE-SOC calculations, but as QSHI in a HSE06-SOC calculation. This reiterates that DGMs identified by DFT can or could actually be found to be QSHIs if studied with techniques, such as many-body perturbation theory, that can correctly estimate the gap, or when exposed to a perturbation.

When considering the QSHIs identified in this work, we obtain a relative abundance of topological insulators of 0.5%, which goes up to 1.4% if the DGMs are included as well. This result is comparable to that of the previous work of Marrazzo *et al.* [12], where an abundance of 1.1% was found for QSHIs. The difference in the values can be explained by two reasons: first, in the work from Marrazzo, strained configurations had also been considered when determining a material topology. Second, when analyzing the space group distributions of the two data sets, shown in Fig. SM1-2, we can observe that the old data set contained more materials with monoclinic Bravais

lattice, in particular with space group 11, which from the analysis seems to be the one with the most QSHIs and DGMs when compared to all other space groups.

IV. CONCLUSIONS

We performed a systematic high-throughput study of 2D exfoliable materials in order to identify QSHIs. Starting from a set of 783 materials, we found four QSHIs and 7 DGMs that could be driven into a QSHI state by material engineering, for a relative abundance of 0.5% for QSHIs and 1.4% if DGMs are also included. Of the four QSHIs identified, the three with the largest gaps had already been explored in the literature. In particular, the two pentatellurides HfTe_5 and ZrTe_5 exhibit both large direct and indirect gaps which make them promising candidates for room-temperature applications. The remaining material, HgNS, represents a QSHI with linear bands in the proximity of its direct gap of 38 meV when computed with a hybrid HSE functional. The main feature of this material is the small gap and band linearity, akin to that of silicene or germanene. For this reason, HgNS could be a promising candidate for future electronic and photonic applications in the low-energy regime.

All materials identified in this work are easily exfoliable, with a binding energy lower than $20 \text{ meV}/\text{\AA}^2$ [18], and for this reason they are prime candidates for possible experimental realization through exfoliation techniques starting from their experimentally known 3D bulk form.

ACKNOWLEDGMENTS

This work was supported by the National Centre for Computational Design and Discovery on Novel Materials (NCCR MARVEL) of the Swiss National Science Foundation. D.G. gratefully acknowledges support from the EU Centre of Excellence, MaX Materials design at the eXascale (Grant No. 824143). We acknowledge PRACE for awarding us access to Marconi at Cineca, Italy (Project No. 2016163963). A.M. and D.C. acknowledge financial support from ICSC - Centro Nazionale di Ricerca in High Performance Computing, Big Data and Quantum Computing, funded by European Union - NextGenerationEU - PNRR, Missione 4 Componente 2 Investimento 1.4 (Grant No. B93C22000620006).

-
- [1] J. Wang and S.-C. Zhang, *Nat. Mater.* **16**, 1062 (2017).
 - [2] Q. Niu, D. J. Thouless, and Y.-S. Wu, *Phys. Rev. B* **31**, 3372 (1985).
 - [3] L. Fu and C. L. Kane, *Phys. Rev. B* **74**, 195312 (2006).
 - [4] A. A. Soluyanov, Topological aspects of band theory, Ph.D. thesis, Rutgers University, 2012.
 - [5] C. L. Kane and E. J. Mele, *Phys. Rev. Lett.* **95**, 146802 (2005).
 - [6] X. Dai, T. L. Hughes, X.-L. Qi, Z. Fang, and S.-C. Zhang, *Phys. Rev. B* **77**, 125319 (2008).
 - [7] C. Timm, *Phys. Rev. B* **86**, 155456 (2012).
 - [8] S. Rachel and M. Ezawa, *Phys. Rev. B* **89**, 195303 (2014).
 - [9] D. A. Abanin, P. A. Lee, and L. S. Levitov, *Solid State Commun.* **143**, 77 (2007).
 - [10] G. J. Ferreira and D. Loss, *Phys. Rev. Lett.* **111**, 106802 (2013).
 - [11] X. Li, Z. Zhang, Y. Yao, and H. Zhang, *2D Mater.* **5**, 045023 (2018).
 - [12] A. Marrazzo, M. Gibertini, D. Campi, N. Mounet, and N. Marzari, *Nano Lett.* **19**, 8431 (2019).
 - [13] T. Olsen, E. Andersen, T. Okugawa, D. Torelli, T. Deilmann, and K. S. Thygesen, *Phys. Rev. Mater.* **3**, 024005 (2019).
 - [14] M. Vergniory, L. Elcoro, C. Felser, N. Regnault, B. A. Bernevig, and Z. Wang, *Nature (London)* **566**, 480 (2019).
 - [15] F. Tang, H. C. Po, A. Vishwanath, and X. Wan, *Nature (London)* **566**, 486 (2019).
 - [16] T. Zhang, Y. Jiang, Z. Song, H. Huang, Y. He, Z. Fang, H. Weng, and C. Fang, *Nature (London)* **566**, 475 (2019).

- [17] M. N. Gjerding, A. Taghizadeh, A. Rasmussen, S. Ali, F. Bertoldo, T. Deilmann, N. R. Knøsgaard, M. Kruse, A. H. Larsen, S. Manti *et al.*, *2D Mater.* **8**, 044002 (2021).
- [18] N. Mounet, M. Gibertini, P. Schwaller, D. Campi, A. Merkys, A. Marrazzo, T. Sohler, I. E. Castelli, A. Cepellotti, G. Pizzi *et al.*, *Nat. Nanotechnol.* **13**, 246 (2018).
- [19] D. Campi, N. Mounet, M. Gibertini, G. Pizzi, and N. Marzari, *ACS Nano* **17**, 11268 (2023).
- [20] G. Shipunov, B. Piening, C. Wuttke, T. Romanova, A. Sadakov, O. Sobolevskiy, E. Y. Guzovsky, A. Usoltsev, V. Pudalov, D. Efremov *et al.*, *J. Phys. Chem. Lett.* **12**, 6730 (2021).
- [21] P.-J. Guo, X.-Q. Lu, W. Ji, K. Liu, and Z.-Y. Lu, *Phys. Rev. B* **102**, 041109(R) (2020).
- [22] C. L. Kane and E. J. Mele, *Phys. Rev. Lett.* **95**, 226801 (2005).
- [23] B. A. Bernevig and S.-C. Zhang, *Phys. Rev. Lett.* **96**, 106802 (2006).
- [24] M. König, S. Wiedmann, C. Brüne, A. Roth, H. Buhmann, L. W. Molenkamp, X.-L. Qi, and S.-C. Zhang, *Science* **318**, 766 (2007).
- [25] L. Fu and C. L. Kane, *Phys. Rev. B* **76**, 045302 (2007).
- [26] G. Giovannetti, P. A. Khomyakov, G. Brocks, P. J. Kelly, and J. van den Brink, *Phys. Rev. B* **76**, 073103 (2007).
- [27] N. D. Drummond, V. Zolyomi, and V. I. Fal'ko, *Phys. Rev. B* **85**, 075423 (2012).
- [28] D. Grassano, O. Pulci, V. O. Shubnyi, S. G. Sharapov, V. P. Gusynin, A. V. Kavokin, and A. A. Varlamov, *Phys. Rev. B* **97**, 205442 (2018).
- [29] J. L. Collins, A. Tadich, W. Wu, L. C. Gomes, J. N. Rodrigues, C. Liu, J. Hellerstedt, H. Ryu, S. Tang, S.-K. Mo *et al.*, *Nature (London)* **564**, 390 (2018).
- [30] C. Zhao, M. Hu, J. Qin, B. Xia, C. Liu, S. Wang, D. D. Guan, Y. Li, H. Zheng, J. Liu, and J. Jia, *Phys. Rev. Lett.* **125**, 046801 (2020).
- [31] J. Liu, T. H. Hsieh, P. Wei, W. Duan, J. Moodera, and L. Fu, *Nat. Mater.* **13**, 178 (2014).
- [32] X. Qian, J. Liu, L. Fu, and J. Li, *Science* **346**, 1344 (2014).
- [33] L. Fu, C. L. Kane, and E. J. Mele, *Phys. Rev. Lett.* **98**, 106803 (2007).
- [34] R.-J. Slager, A. Mesaros, V. Juričić, and J. Zaanen, *Nat. Phys.* **9**, 98 (2013).
- [35] J. Kruthoff, J. de Boer, J. van Wezel, C. L. Kane, and R.-J. Slager, *Phys. Rev. X* **7**, 041069 (2017).
- [36] H. C. Po, A. Vishwanath, and H. Watanabe, *Nat. Commun.* **8**, 1 (2017).
- [37] E. Khalaf, H. C. Po, A. Vishwanath, and H. Watanabe, *Phys. Rev. X* **8**, 031070 (2018).
- [38] Z. Song, T. Zhang, Z. Fang, and C. Fang, *Nat. Commun.* **9**, 3530 (2018).
- [39] D. Campi, N. Mounet, M. Gibertini, G. Pizzi, and N. Marzari, Materials Cloud two-dimensional crystals database (MC2D), <https://doi.org/10.24435/materialscloud:36-nd> (2022).
- [40] R. Gillen, S. J. Clark, and J. Robertson, *Phys. Rev. B* **87**, 125116 (2013).
- [41] P. Giannozzi, S. Baroni, N. Bonini, M. Calandra, R. Car, C. Cavazzoni, D. Ceresoli, G. L. Chiarotti, M. Cococcioni, I. Dabo, A. D. Corso, S. de Gironcoli, S. Fabris, G. Fratesi, R. Gebauer, U. Gerstmann, C. Gougoussis, A. Kokalj, M. Lazzeri, L. Martin-Samos *et al.*, *J. Phys.: Condens. Matter* **21**, 395502 (2009).
- [42] P. Giannozzi, O. Andreussi, T. Brumme, O. Bunau, M. B. Nardelli, M. Calandra, R. Car, C. Cavazzoni, D. Ceresoli, M. Cococcioni *et al.*, *J. Phys.: Condens. Matter* **29**, 465901 (2017).
- [43] J. P. Perdew, K. Burke, and M. Ernzerhof, *Phys. Rev. Lett.* **77**, 3865 (1996).
- [44] D. R. Hamann, *Phys. Rev. B* **88**, 085117 (2013).
- [45] M. van Setten, M. Giantomassi, E. Bousquet, M. Verstraete, D. Hamann, X. Gonze, and G.-M. Rignanese, *Comput. Phys. Commun.* **226**, 39 (2018).
- [46] D. Gresch, G. Autes, O. V. Yazyev, M. Troyer, D. Vanderbilt, B. A. Bernevig, and A. A. Soluyanov, *Phys. Rev. B* **95**, 075146 (2017).
- [47] C. Sgierovello, M. Peressi, and R. Resta, *Phys. Rev. B* **64**, 115202 (2001).
- [48] J. Heyd, G. E. Scuseria, and M. Ernzerhof, *J. Chem. Phys.* **118**, 8207 (2003).
- [49] G. Bergerhoff, R. Hundt, R. Sievers, and I. D. Brown, *J. Chem. Inf. Comput.* **23**, 66 (1983).
- [50] D. Zagorac, H. Müller, S. Ruehl, J. Zagorac, and S. Rehme, *J. Appl. Crystallogr.* **52**, 918 (2019).
- [51] S. Gražulis, A. Daškevič, A. Merkys, D. Chateigner, L. Lutterotti, M. Quiros, N. R. Serebryanaya, P. Moeck, R. T. Downs, and A. Le Bail, *Nucleic Acids Res.* **40**, D420 (2012).
- [52] P. Villars, M. Berndt, K. Brandenburg, K. Cenzual, J. Daams, F. Hulliger, T. Massalski, H. Okamoto, K. Osaki, A. Prince *et al.*, *J. Alloys Compd.* **367**, 293 (2004).
- [53] A. A. Soluyanov and D. Vanderbilt, *Phys. Rev. B* **83**, 235401 (2011).
- [54] G. Pizzi, V. Vitale, R. Arita, S. Blügel, F. Freimuth, G. Géranton, M. Gibertini, D. Gresch, C. Johnson, T. Koretsune *et al.*, *J. Phys.: Condens. Matter* **32**, 165902 (2020).
- [55] S. Baroni, S. De Gironcoli, A. Dal Corso, and P. Giannozzi, *Rev. Mod. Phys.* **73**, 515 (2001).
- [56] G. Pizzi, A. Cepellotti, R. Sabatini, N. Marzari, and B. Kozinsky, *Comput. Mater. Sci.* **111**, 218 (2016).
- [57] S. Huber, S. Zoupanos, M. Uhrin, L. Talirz, L. Kahle, R. Häuselmann, D. Gresch, T. Müller, A. V. Yakutovich, C. W. Andersen *et al.*, *Scientific Data* **7**, 300 (2020).
- [58] D. Grassano, D. Campi, A. Marrazzo, and N. Marzari, 2D topological insulators, <https://www.materialscloud.org/discover/2dtopo> (2022).
- [59] Y. Hinuma, G. Pizzi, Y. Kumagai, F. Oba, and I. Tanaka, *Comput. Mater. Sci.* **128**, 140 (2017).
- [60] See Supplemental Material at <http://link.aps.org/supplemental/10.1103/PhysRevMaterials.7.094202> for the atomic structure, band structure, density of states, and HWCC evolution (where applicable) of the QSHIs and DGMs identified which include Refs. [12,75].
- [61] G. M. Gusev, Z. D. Kvon, E. B. Olshanetsky, A. D. Levin, Y. Krupko, J. C. Portal, N. N. Mikhailov, and S. A. Dvoretzky, *Phys. Rev. B* **89**, 125305 (2014).
- [62] F. Aryasetiawan and O. Gunnarsson, *Rep. Prog. Phys.* **61**, 237 (1998).
- [63] T. V. Menshchikova, M. Otrokov, S. Tsirkin, D. Samorokov, V. Bebnava, A. Ernst, V. Kuznetsov, and E. V. Chulkov, *Nano Lett.* **13**, 6064 (2013).
- [64] Y. Liu, Y. Li, S. Rajput, D. Gilks, L. Lari, P. Galindo, M. Weinert, V. Lazarov, and L. Li, *Nat. Phys.* **10**, 294 (2014).
- [65] L. Zhou, L. Kou, Y. Sun, C. Felser, F. Hu, G. Shan, S. C. Smith, B. Yan, and T. Frauenheim, *Nano Lett.* **15**, 7867 (2015).

- [66] M. Hirayama, S. Matsuishi, H. Hosono, and S. Murakami, *Phys. Rev. X* **8**, 031067 (2018).
- [67] L. Zhou, B. Shao, W. Shi, Y. Sun, C. Felser, B. Yan, and T. Frauenheim, *2D Mater.* **3**, 035022 (2016).
- [68] Z.-Q. Huang, W.-C. Chen, G. M. Macam, C. P. Crisostomo, S.-M. Huang, R.-B. Chen, M. A. Albao, D.-J. Jang, H. Lin, and F.-C. Chuang, *Nanoscale Res. Lett.* **13**, 1 (2018).
- [69] H. Weng, X. Dai, and Z. Fang, *Phys. Rev. X* **4**, 011002 (2014).
- [70] N. D. Lowhorn, T. M. Tritt, E. E. Abbott, and J. Kolis, *Appl. Phys. Lett.* **88**, 022101 (2006).
- [71] A. O'Hare, F. Kusmartsev, and K. Kugel, *Nano Lett.* **12**, 1045 (2012).
- [72] A. Marrazzo, M. Gibertini, D. Campi, N. Mounet, and N. Marzari, *Phys. Rev. Lett.* **120**, 117701 (2018).
- [73] J. Liu, H. Wang, C. Fang, L. Fu, and X. Qian, *Nano Lett.* **17**, 467 (2017).
- [74] A. Wang, Z. Wang, A. Du, and M. Zhao, *Phys. Chem. Chem. Phys.* **18**, 22154 (2016).
- [75] K. Momma and F. Izumi, *J. Appl. Crystallogr.* **44**, 1272 (2011).